DOI: 10.31276/VJSTE.2025.0050

Effect of chemical modification on the superhydrophobic properties of CT3 steel surfaces

Nguyen Van Kiet, Pham Dinh Hai, Phan Minh Quoc Binh, Nguyen Thi Phuong Nhung*

PetroVietnam University, 762 Cach Mang Thang Tam Street, Ba Ria Ward, Ho Chi Minh City, Vietnam

Received 26 June 2025; revised 8 July 2025; accepted 8 August 2025

Abstract:

This study systematically explores the influence of diverse chemical surface modifications on the water-repellent properties of CT3 steel substrates, focusing on the synergistic relationship between surface topography and chemical composition in realising superhydrophobic behaviour. Initially, steel samples were coated with a ZnO layer to significantly enhance surface roughness, serving as a foundation for subsequent chemical treatments. The surfaces were then functionalised with various low-surface-energy agents, including triethoxymethylsilane (MTES), polydimethylsiloxane (PDMS), 1H,1H,2H,2H-perfluorooctyltriethoxysilane (PFOS), stearic acid (SA), and high-density polyethylene (HDPE). Quantitative assessment via contact angle measurements demonstrated that coatings of MTES, PFOS, PDMS, and SA successfully achieved superhydrophobicity, characterised by water contact angles greater than 150° and minimal contact angle hysteresis. Of particular interest, MTES treatment in toluene solvent not only effectively reduced the surface free energy but also promoted the formation of nanofilamentous microstructures, thereby amplifying surface roughness and hydrophobic performance. The chemically and morphologically modified surfaces were thoroughly characterised using scanning electron microscopy (SEM), Fourier-transform infrared spectroscopy (FTIR), and detailed wettability analyses to correlate surface structure with hydrophobicity.

Keywords: **anti-corrosion, low energy surface, steel surface, superhydrophobic steel surface.**

Classification numbers: **2.2, 2.3**

1. Introduction

Corrosion remains a major challenge in the oil and gas industry, as it directly affects pipeline integrity and reduces operational efficiency. One promising strategy for corrosion mitigation is the application of superhydrophobic surfaces, defined by water contact angles greater than 150°. These surfaces not only repel water effectively but also possess self-cleaning properties, limiting the buildup of corrosive substances. By reducing liquid-solid contact, superhydrophobic coatings enhance corrosion resistance and contribute to the overall safety and reliability of pipeline systems. Furthermore, their use supports sustainability by potentially decreasing the environmental risks associated with oil leaks from corroded or damaged pipelines [1-3].

To achieve superhydrophobicity on steel surfaces, researchers typically combine surface chemical modification with micro- and nanostructuring techniques. Common fabrication methods include wet- and dry-etching, sol-gel processing, electrochemical deposition, hydrothermal synthesis and chemical vapour deposition. Among these techniques, reducing surface energy - often through the application of low-surface-energy polymer coatings or silanisation - is widely employed to enhance hydrophobic behaviour [2-8].

For example, Y. Miao, et al. (2020) [9] demonstrated that the self-polymerisation of dopamine (DA) on 316L stainless steel resulted in the formation of nanoscale particles, approximately 80-100 nm in diameter, on the steel surface. Subsequent functionalisation of the polydopamine (PDA) film with 1H,1H,2H,2H-perfluorodecanethiol (PFDT) produced a fluorinated polydopamine (fPDA) coating, which significantly enhanced both superhydrophobicity and corrosion resistance. Similarly, N.V. Motlagh, et al. (2013) [10] successfully fabricated a superhydrophobic steel surface by integrating a silica multilayer structure (~11 µm thick) with silanisation using 1H,1H,2H,2H-perfluorodecyltriethoxysilane. This approach achieved a water contact angle of approximately 157° and a maximum corrosion protection efficiency of 97.33%. While these approaches have been successful on stainless steel and other alloys, systematic studies focusing on CT3 steel - an economical and widely used carbon steel - remain limited. Moreover, few works have directly compared the effects of different low-surface-energy materials under similar surface-roughness conditions to isolate their contribution to superhydrophobicity and corrosion protection.

Building upon these findings, our previous study introduced a simple yet effective approach for fabricating superhydrophobic surfaces on CT3 steel [11-12]. The present work expands upon this foundation by providing a comprehensive comparison of five

*Corresponding author: Email: nhungntp@pvu.edu.vn

different chemical modifiers - MTES, PDMS, PFOS, SA and HDPE - applied under controlled structural conditions. We specifically examine how each modifier influences surface morphology, water repellency and the potential formation of nanostructures.

This comparative approach represents a novel contribution to the field by isolating the chemical treatment variable while holding structural parameters constant, thereby providing clearer insights into the role of surface chemistry in achieving durable superhydrophobicity on CT3 steel. These findings are intended to guide the rational design of superhydrophobic coatings for low-cost steels used in corrosive environments.

2. Materials and methods

2.1. Materials

Triethoxymethylsilane, polydimethylsiloxane, and 1H,1H,2H,2H-perfluorooctyltriethoxysilane were obtained from Sigma-Aldrich. Other substances, such as ethanol, acetone, H_2SO_4, H_2O_2, NH_3, $Zn(CH_3COO)_2$, high density polyethylene, and stearic acid, were purchased from Xilong Company. CT3 steel substrates were sourced from China. All materials were used as received without further purification.

2.2. Preparation of superhydrophobic steel surface

The chemical modifiers in this study were selected on the basis of their low surface energy, molecular structure and affinity for ZnO-coated steel. MTES and PFOS afford strong bonding and introduce fluorinated or alkyl chains, whereas PDMS and SA provide flexible hydrophobic moieties. HDPE was included to assess the influence of a bulk hydrophobic polymer. These compounds have been widely reported to reduce surface energy and enhance water repellency, thereby enabling a comparative evaluation of their effects on the superhydrophobic properties of CT3 steel.

2.2.1. Formation of micro- and nanostructured ZnO coating

Prior to chemical modification, the CT3 steel substrate was coated with a micro- and nanostructured ZnO layer; further details of the coating procedure are available in our previous publications [11, 12]. The steel surfaces were cut to dimensions of 1.5×3.0×3.0 cm, polished sequentially with 100, 200 and 600-grit sandpapers, degreased in acetone and ethanol, and finally rinsed with distilled water.

A two-electrode electrochemical cell was employed, with the CT3 steel substrate serving as the cathode and a zinc sheet (0.2×2×5 cm) as the anode. Deionised water was used as the electrolyte. A constant voltage of 1 V was applied for 45 minutes to promote zinc deposition on the steel surface. Following electrolysis, the substrate was rinsed with deionised water, dried, and annealed at 250°C for 120 minutes to convert the zinc layer into a ZnO thin film. The resulting substrate is hereafter referred to as ZnO-coated- CT3.

2.2.2. Chemical modification

The ZnO-coated steel substrates were subjected to UV/O_3 treatment for 30 minutes to remove organic contaminants and generate surface hydroxyl (-OH) groups, thereby activating the surface (Fig. 1). Subsequently, each low-surface-energy material was applied to the activated substrates. The resulting samples are hereafter referred to as OH-ZnO coated-CT3 surfaces.

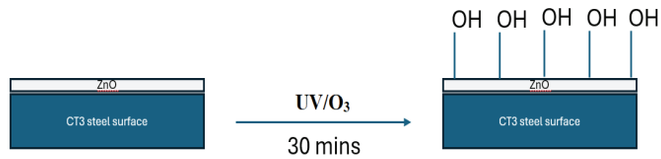

Fig. 1. Mechanism of surface activation by formation of hydroxyl (-OH) groups on the ZnO layer surface.

Polydimethylsiloxane coating: The activated ZnO coated-CT3 substrates were immersed in a solution of PDMS (0.01 $g.ml^{-1}$) and curing agent (0.001 $mg.ml^{-1}$) for 10 minutes (Fig. 2). Following immersion, the samples were dried at 120°C for 2 hours to complete curing. The PDMS employed in this study comprised dimethyl siloxane (dimethylvinyl-terminated), dimethylvinylated and trimethylated silica, and tetra(dimethylsiloxy)silane. The resulting substrates are hereafter referred to as PDMS-ZnO coated-CT3.

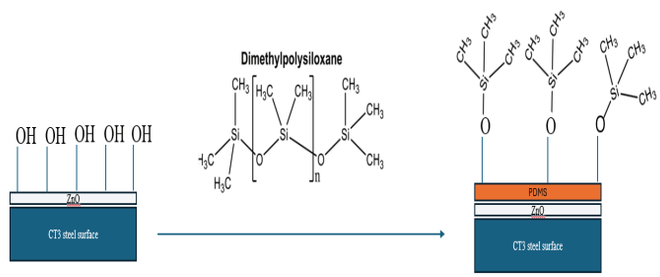

Fig. 2. Mechanism of polydimethylsiloxane coating.

High-density polyethylene coating: The activated ZnO coated-CT3 substrates were immersed for 3 minutes in a 0.01 $g.ml^{-1}$ solution of HDPE in toluene, maintained at 78°C (Fig. 3). After immersion, the samples were dried at room temperature in a fume hood. The resulting substrates are hereafter referred to as HDPE-ZnO coated-CT3.

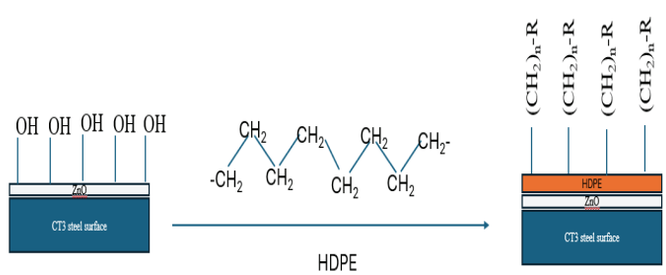

Fig. 3. Mechanism of high-density polyethylene coating.

Silanisation with perfluorosilane: Further details of the silanisation process are available in our previous publication [11]. The activated ZnO coated-CT3 substrates were immersed in a hexane solution containing 3 mM PFOS. After immersion,

the substrates were rinsed three times with hexane and then three times with ethanol, before being dried under a gentle flow of nitrogen. The resulting substrates are hereafter referred to as PFOS-ZnO coated-CT3.

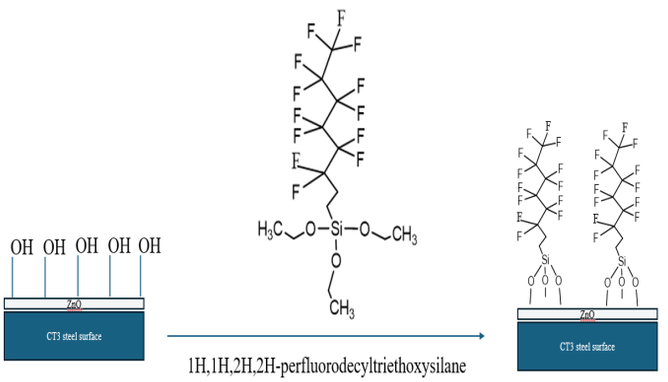

Fig. 4. Mechanism of perfluorosilane coating.

The mechanism of PFOS modification is illustrated in Fig. 4. During the process, PFOS undergoes hydrolysis to generate -OH groups, which then react with hydroxyl groups on the ZnO surface. This reaction facilitates the covalent attachment of $-CF_3$-terminated fluorinated chains onto the ZnO coated-CT3 substrate, thereby reducing surface energy and enhancing hydrophobicity

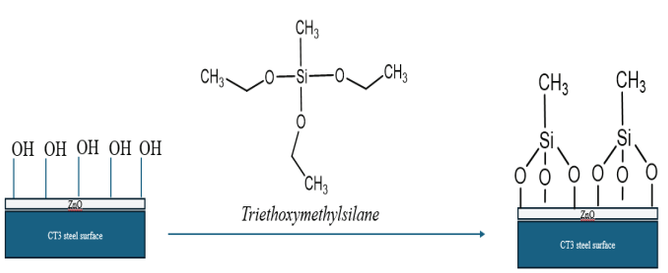

Fig. 5. Mechanism of triethoxymethylsilane modification in ethanol.

The mechanism of MTES modification is illustrated in Fig. 5. During silanisation, MTES undergoes hydrolysis to yield -OH groups, which subsequently react with surface hydroxyl groups on the ZnO layer. This reaction results in the covalent attachment of $-CH_3$ groups to the surface, thereby lowering surface energy and enhancing hydrophobicity.

Nanofilament coating: The activated ZnO coated-CT3 substrates were immersed in a toluene solution containing 5 mM MTES and 0.18 mM HCl for 8 hours. After treatment, the substrates were rinsed three times with toluene, followed by three rinses with ethanol, and then dried under a gentle flow of nitrogen. The resulting substrates are hereafter referred to as Nanofilament-ZnO coated-CT3.

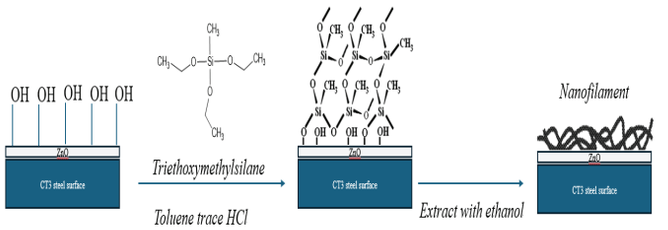

Fig. 6. Mechanism of triethoxymethylsilane modification in toluene.

The proposed mechanism of surface modification in toluene is illustrated in Fig. 6. In the nonpolar toluene solvent, a sol-gel process occurs in which MTES serves as a precursor for silica (SiO_2) formation, catalysed by HCl. The low polarity of toluene affects the sol-gel reaction rate by limiting the solubility of MTES and associated reactants, thereby promoting phase separation or aggregation. This environment facilitates the formation of filament-like silica structures as the silica phase precipitates onto the CT3 surface. Consequently, MTES-based modification in toluene alters both the surface morphology and chemical composition of the ZnO coated-CT3 substrate.

Stearic acid modification: The activated ZnO coated-CT3 substrates were immersed in a 0.01 M solution of stearic acid in ethanol for 3 hours. Following immersion, the substrates were rinsed three times with ethanol and then dried at room temperature. The resulting substrates are hereafter referred to as SA-ZnO coated-CT3.

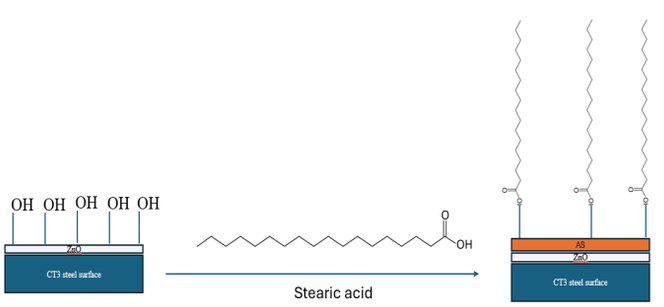

Fig. 7. Mechanism of stearic acid modification in ethanol.

The proposed mechanism of modification is illustrated in Fig. 7. During the process, surface hydroxyl (-OH) groups on the ZnO layer react with the carboxylic acid (-COOH) groups of stearic acid. This reaction results in the covalent attachment of long hydrocarbon chains onto the surface, effectively lowering its surface energy and enhancing hydrophobicity.

2.3. Sample characterisation

Surface characterisation: The morphology of the steel surfaces was examined by scanning electron microscopy (SEM; JEOL 7600F) equipped with energy-dispersive X-ray spectroscopy (EDS; Oxford Instruments). Fourier-transform infrared spectroscopy (FTIR) was employed to confirm successful grafting

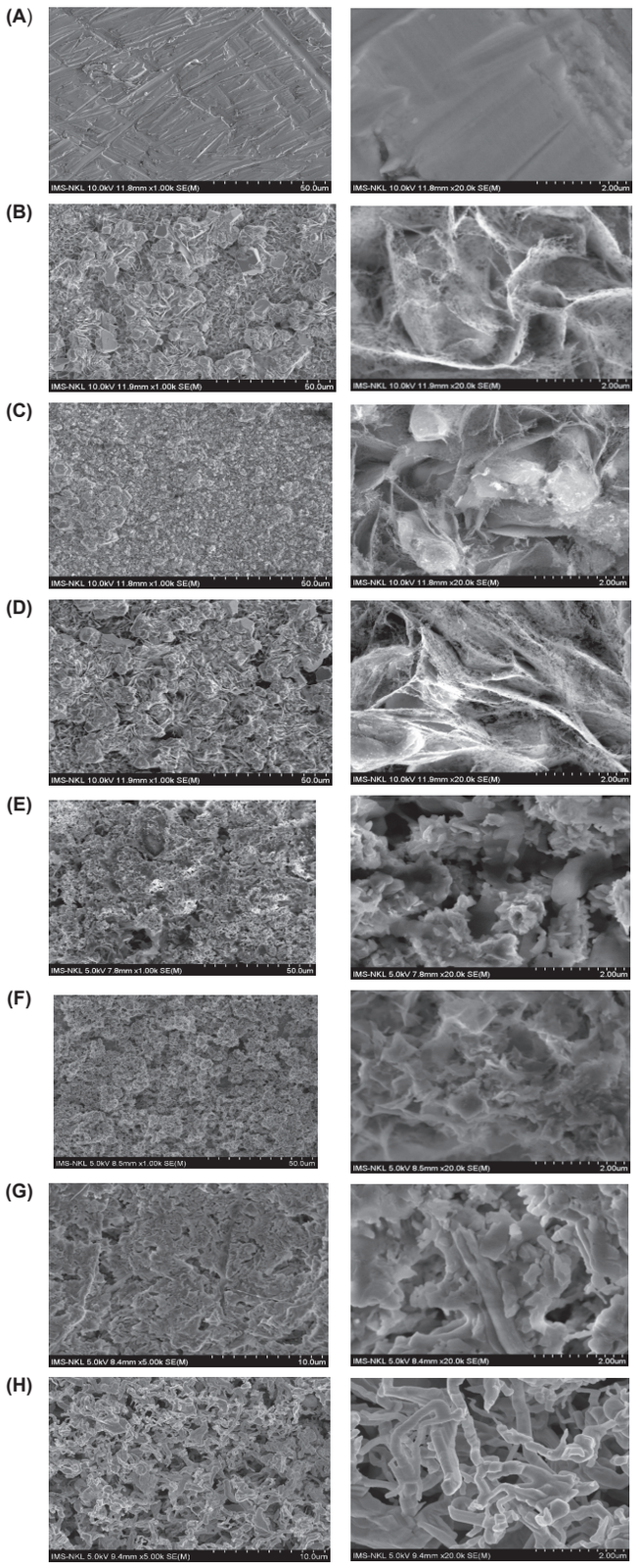

Fig. 8. The SEM images. (A) Steel surface; **(B)** ZnO coated steel surface with silanisation; **(C)** MTES-ZnO coated-CT3; **(D)** PFOS-ZnO coated-CT3; **(E)** SA-ZnO coated-CT3; **(F)** PDMS-ZnO coated-CT3; **(G)** HDPE-ZnO coated-CT3; **(H)** Nanofilament-ZnO coated-CT3.

of the chemical modifiers onto the ZnO-coated substrates. Wetting behaviour was evaluated by measuring the static water contact angle using an OCA goniometer (DataPhysics). For each sample, three measurements were taken at different positions using a 5 µl droplet of distilled water to ensure reproducibility.

3. Results and discussion

As shown in the SEM images (Figs. 8A and 8B), the polished steel surface exhibits numerous scratches, whereas the ZnO-coated steel surface appears markedly more porous and rough. This increased surface roughness constitutes one of the two essential factors for achieving superhydrophobicity [5].

Chemical modification of the ZnO-coated steel with PFOS and MTES (in methanol solution) alters only the surface chemistry, without appreciably affecting the underlying ZnO morphology (Figs. 8C and 8D); thus, the original coating structure is preserved [8-9]. In contrast, treatments with HDPE, PDMS, SA or MTES in toluene induce changes in both chemical composition and surface topography (Figs. 8E, 8F, 8G and 8H), indicating a combined chemical and structural transformation.

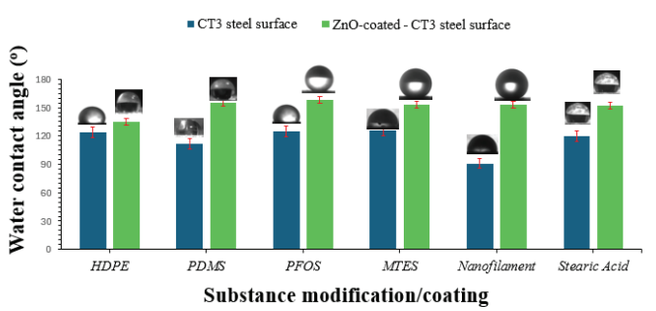

Fig. 9. Wetting properties of substrates: steel substrate, ZnO coated-CT3 substrate with chemical modification (HDPE, PDMS, PFOS, MTES, Nanofilament, stearic acid).

In this study, both bare and ZnO coated-CT3 steel surfaces were subjected to UV/O_3 treatment prior to chemical modification. Water contact angle (WCA) measurements were used to evaluate wetting behaviour and assess the effectiveness of the chemical functionalisation (Fig. 9). The results indicate that chemical treatment induced a transition from hydrophilic to hydrophobic states (WCA>90°) on both surface types. Notably, the ZnO-coated surfaces exhibited slightly higher WCA values than their uncoated counterparts, with a difference of less than 10°. This enhancement is attributed to the increased surface roughness introduced by the hierarchical micro- and nanostructured ZnO layer, which amplifies water-repellent behaviour.

Following ZnO deposition, chemical modification with low-surface-energy compounds such as PDMS, PFOS, MTES and SA yielded superhydrophobic surfaces, characterised by WCA values exceeding 150° and low contact-angle hysteresis (<2°), indicative of minimal water adhesion and excellent self-cleaning performance. In contrast, surfaces modified with HDPE exhibited only moderate hydrophobicity (WCA≈135°), likely due to its

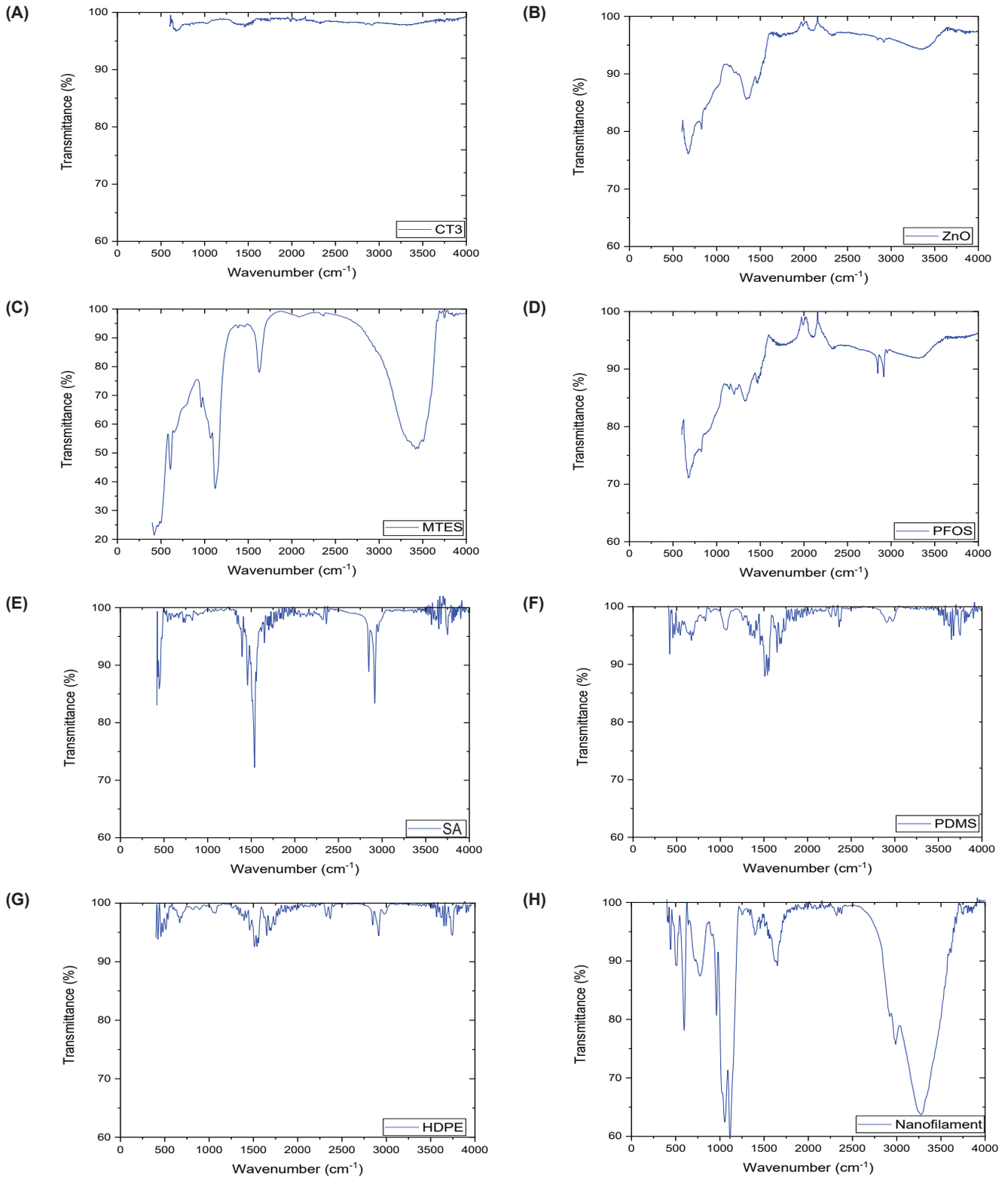

Fig. 10. Transmission Fourier-transform infrared spectroscopy spectrum. (A) Steel surface (CT3); **(B)** ZnO coated steel surface with silanisation; **(C)** MTES-ZnO coated-CT3; **(D)** PFOS- ZnO coated-CT3; **(E)** SA-ZnO coated-CT3; **(F)** PDMS-ZnO coated-CT3; **(G)** HDPE-ZnO coated-CT3; and **(H)** Nanofilament-ZnO coated-CT3.

relatively higher surface energy and partial occlusion of the porous ZnO structure, which reduces air retention within surface cavities.

The observed water-repellent properties can be explained by the combined contributions of hierarchical surface roughness, reduced surface energy and interfacial air entrapment. Specifically, the ZnO nanostructures increase surface roughness, facilitating the formation of air pockets beneath the liquid droplet. Concurrently, the application of low-surface-energy molecules reduces solid-liquid interfacial tension. This dual effect stabilises a Cassie-Baxter wetting regime, in which the liquid is suspended atop a composite interface of solid and trapped air, resulting in high apparent contact angles and low adhesion.

The surface energies of the applied coatings varied significantly. PFOS exhibited the lowest surface energy (~10-12 $mN.m^{-1}$), followed by MTES, PDMS and SA (20-25 $mN.m^{-1}$), while HDPE presented the highest (~31-33 $mN.m^{-1}$). Coatings with surface energies below 25 $mN.m^{-1}$ consistently facilitated superhydrophobic behaviour. Among the tested materials, stearic acid is noteworthy for its low cost, non-toxicity and ease of processing, making it a promising candidate for scalable fabrication of water-repellent steel surfaces. In contrast, silane-based compounds and PDMS, while effective, may be less favourable due to higher cost and potential environmental concerns.

By comparing the FTIR spectrum of the uncoated-CT3 substrate (Fig. 10A) with that of the ZnO-coated CT3 substrate (Fig. 10B), a new absorption band emerges in the 900-700 cm-1 region after ZnO coating. This band is attributed to Zn-O bond vibrations, confirming the successful formation of a ZnO layer on the steel surface [13].

Following modification with triethoxymethylsilane (MTES) (Fig. 10C), the FTIR spectrum exhibits a characteristic Si-CH_3 absorption band at ~1274 cm^{-1}, alongside weaker C-H stretching signals between 2900 and 2980 cm^{-1}. A broad, intense absorption in the 1000-1150 cm^{-1} region is attributed to Si-O-Si polysiloxane network formation and possibly to Si-O-Zn interfacial bonding, indicating successful hydrolysis and condensation of MTES [14]. A broad -OH band centred near 3400 cm^{-1} reflects the presence of adsorbed water or residual surface hydroxyl groups.

Subsequent modification with PFOS (Fig. 10D) introduces strong absorption bands in the 1100-1350 cm^{-1} and 2850-2980 cm^{-1} regions, corresponding to C-F and C-H stretching vibrations, respectively [15]. Signals between 1000 and 1100 cm^{-1} confirm the formation of Si-O-Zn or Si-O-Si bonds, verifying the stable attachment of the fluorinated silane layer.

After treatment with SA (Fig. 10E), new peaks appear at 2954, 2915 and 2847 cm^{-1}, attributed to C-H stretching in long hydrocarbon chains. A peak at 1794 cm^{-1} indicates C=O stretching, suggesting the presence of carboxylic or ester groups. Additional bands at 1651 cm^{-1} and 1558 cm^{-1} may relate to C=C or C-O stretching, confirming chemical interaction with the surface. Bending and rocking vibrations of -CH_2- and -CH_3 groups are observed at 1457, 1395, 823 and 721 cm^{-1}, indicating successful grafting of SA [16].

For the PDMS-coated sample (Fig. 10F), strong Si-O-Si stretching bands appear at 1142 and 1068 cm^{-1}, characteristic of polydimethylsiloxane. C-H stretching vibrations at 2960 and 2908 cm^{-1} correspond to -CH_3 and -CH_2- groups [17]. A distinct band at 1260 cm^{-1} confirms Si-CH_3 bonds, while peaks at 891 and 828 cm^{-1} indicate Si-C bonds. Absorptions between 734 and 669 cm^{-1} are associated with siloxane backbone vibrations.

In the case of the HDPE-coated surface (Fig. 10G), absorption bands at 2913 and 2847 cm^{-1} are consistent with -CH_2- stretching vibrations typical of polyethylene. Bending vibrations are observed at 1458 and 1379 cm^{-1} [18]. Although a characteristic HDPE band near 720 cm^{-1} is expected, it is not clearly distinguishable in the spectrum.

Finally, the FTIR spectrum of the silicon nanofilament-coated sample (Fig. 10H) exhibits a strong absorption band in the 1000-1100 cm^{-1} range, indicative of Si-O-Si bond formation typical of silica networks. A broad band from 3300 to 3600 cm^{-1} corresponds to Si-OH stretching, suggesting surface hydration or water adsorption. A weak band between 600 and 700 cm^{-1} is assigned to Si-Si bonding, while peaks below 500 cm^{-1} may be associated with crystalline silicon features.

4. Conclusions

In this study, superhydrophobic steel surfaces were successfully fabricated by combining micro-/nanostructuring via ZnO deposition with subsequent chemical modification using low-surface-energy materials. The experimental results highlight the pivotal role of chemical surface treatment in achieving superhydrophobicity. All ZnO coated surfaces modified with MTES, PFOS, PDMS and SA exhibited water contact angles above 150° with low contact-angle hysteresis, confirming the formation of stable superhydrophobic states. In contrast, HDPE-modified surfaces displayed only moderate hydrophobicity, attributable to their higher surface energy and reduced capacity to retain hierarchical porosity.

A key finding is the exceptional effectiveness of MTES in toluene, which not only lowered surface energy but also promoted the formation of nanofilament structures, thereby enhancing surface roughness and water repellency. This dual effect underscores the synergistic interplay between hierarchical topography and surface chemistry in stabilising the Cassie-Baxter wetting regime.

The novelty of this work lies in the systematic comparison of multiple surface modifiers on ZnO-coated steel and the demonstration that surface morphology can be actively tuned during chemical treatment to further enhance hydrophobicity. These insights provide a scientific basis for the rational design of superhydrophobic coatings on steel substrates and suggest significant potential for practical applications in corrosion protection, anti-fouling and self-cleaning materials.

CRediT author statement

Nguyen Van Kiet, Pham Dinh Hai: Image preparation, Conducting experiments; Phan Minh Quoc Binh: Literature review. Nguyen Thi Phuong Nhung: Literature review, Conceptualisation, Data analysis, Conducting experiments, Writing - Reviewing, and Editing.

ACKNOWLEDGEMENTS

The current project was financially supported by PetroVietnam University under grant code GV2303.

COMPETING INTERESTS

The authors declare that there is no conflict of interest regarding the publication of this article.

REFERENCES

[1] M. Jin, Q. Xing, Z. Chen (2020), "A review: Natural superhydrophobic surfaces and applications", *J. Biomater. Nanobiotechnol.*, **11(2)**, pp.110-149, DOI: 10.4236/jbnb.2020.112008.

[2] T.P. Rasitha, N.G. Krishna, B. Anandkumar, et al. (2024), "A comprehensive review on anticorrosive/antifouling superhydrophobic coatings: Fabrication, assessment, applications, challenges and future perspectives", *Advances in Colloid and Interface Science*, **324**, DOI: 10.1016/j.cis.2024.103090.

[3] C. Du, X. He, F. Tian, et al. (2019), "Preparation of superhydrophobic steel surfaces with chemical stability and corrosion", *Coatings*, **9(6)**, DOI: 10.3390/coatings9060398.

[4] J.T. Simpson, S.R. Hunter, T. Aytug (2015), "Superhydrophobic materials and coatings: A review", *Reports Prog. Phys.*, **78(8)**, DOI: 10.1088/0034-4885/78/8/086501.

[5] T.P.N. Nguyen, P. Brunet, Y. Coffinier, et al. (2010), "Quantitative testing of robustness on superomniphobic surfaces by drop impact", *Langmuir*, **26(23)**, pp.18369-18373, DOI: 10.1021/la103097y.

[6] J. Qi, S. Li, X. Guo, et al. (2025), "Advancements in superhydrophobic foam materials for efficient oil-water separation: Modification techniques and future applications", *Journal of Water Process Engineering*, **70**, DOI: 10.1016/j.jwpe.2025.107008.

[7] Y. Guo, W. Li, L. Zhu, et al. (2012), "Phosphoric chemical conversion coating with excellent wax-repellent performance", *Appl. Surf. Sci.*, **259**, pp.356-361, DOI: 10.1016/j.apsusc.2012.07.051.

[8] D. Wang, Q. Sun, M.J. Hokkanen, et al. (2020), "Design of robust superhydrophobic surfaces", *Nature*, **582**, pp.55-59, DOI: 10.1038/s41586-020-2331-8.

[9] Y. Miao, D. Zhang, N. Cao, et al. (2020), "Mussel-inspired superhydrophobic surfaces on 316L stainless steel with enhanced corrosion resistance", *Metall. Mater. Trans. A Phys. Metall. Mater. Sci.*, **51(2)**, pp.909-919, DOI: 10.1007/s11661-019-05573-7.

[10] N.V. Motlagh, F.C. Birjandi, J. Sargolzaei, et al. (2013), "Durable, superhydrophobic, superoleophobic and corrosion resistant coating on the stainless steel surface using a scalable method", *Appl. Surf. Sci.*, **283**, pp.636-647, DOI: 10.1016/j.apsusc.2013.06.160.

[11] N.T.P. Nhung, N.V. Chien, N.D. Nam, et al. (2016), "Simple method to fabricate superhydrophobic carbon steel surface", *Petrovietnam J.*, **10**, pp.44-47.

[12] T.P.N. Nguyen, T.N.T. Nguyen, H.L. Nguyen, et al. (2022), "Micro/nanostructured ZnO-based superhydrophobic steel surface with enhanced corrosion protection", *Petrovietnam J.*, **6**, pp.59-66, DOI: 10.47800/pvj.2022.06-07.

[13] B. John, P.R. Rajimol, T.P.D. Rajan, et al. (2022), "Design and fabrication of nano textured superhydrophobic and anti-corrosive silane-grafted ZnO/bio-based polyurethane bilayer coating", *Surf. Coatings Technol.*, **451**, DOI: 10.1016/j.surfcoat.2022.129036.

[14] K. Ma, X.L. Cai, H. Yin, et al. (2025), "Superhydrophobic composite coatings with thermal stability for oil/water separation", *Materials Today Communications*, **44**, DOI: 10.1016/j.mtcomm.2025.111907.

[15] M. Saget, N. Nuns, P. Supiot, et al. (2023), "Ultra-hydrophobic biomimetic transparent bilayer thin film deposited by atmospheric pressure plasma", *Surfaces and Interfaces*, **42**, DOI: 10.1016/j.surfin.2023.103398.

[16] T. Liang, H. Yuan, C. Li, et al. (2020), "Corrosion inhibition effect of nano-SiO_2 for galvanized steel superhydrophobic surface", *Surf. Coatings Technol.*, **406**, DOI: 10.1016/j.surfcoat.2020.126673.

[17] Y. Wei, Y. Hu, Z. Liang, et al. (2025), "PDMS@SiO_2 surface modified superhydrophobic melamine sponges for enhanced drag reduction", *Surf. Coatings Technol.*, **509**, DOI: 10.1016/j.surfcoat.2025.132200.

[18] A. Blanco, R. Juan, B. Paredes, et al. (2025), "Advancing polypropylene quantification in recycled HDPE: A comparative study of FTIR, DSC, TREF, and TGIC for enhanced plastic circularity", *Polym. Test.*, **149**, DOI: 10.1016/j.polymertesting.2025.108855.